



Modal response identification of a highway bridge under traffic loads using frequency domain decomposition (FDD)

Mehmet Akköse^{a,*}, Hugo C. Gomez^b, Maria Q. Feng^c

^a Karadeniz Technical University, Department of Civil Engineering, 61080 Trabzon, Turkey

^b Holmes Culley, 235 Montgomery Street, Suite 1250, San Francisco, CA 94104, USA

^c Department of Civil Engineering and Engineering Mechanics, Columbia University, New York, NY 10027, USA

ABSTRACT

In this study, a four-span, 224m long, post-tensioned concrete box girder bridge supported on single column piers was subject to a series of controlled vehicle tests. Bridge acceleration response datasets were used to study the effect of truck speed and a sudden stop, on the modal identification of the bridge structure. Natural frequencies and mode shapes of the bridge were determined using the frequency domain decomposition technique for all datasets. The passing of the truck rendered difficult to identify the first bridge frequency. Conversely, the vehicle tests improved the identification of higher vibration modes. This is because the truck preferentially excites the bridge vertical response, which is associated with higher modes of vibrations, especially when a sudden stop of the vehicle occurs. Thus, carefully conducted vehicle-crossing tests provide detailed information about the bridge structure dynamics in the vertical direction. However, to identify lower modes, no vehicle on the bridge is preferred.

ARTICLE INFO

Article history:

Received 6 February 2017

Revised 12 March 2017

Accepted 17 March 2017

Keywords:

Box girder bridge

Modal identification

Frequency domain decomposition

Traffic loads

1. Introduction

Bridges in service are subject to a combination of various external loads, among which traffic loads are constantly imposed on the bridge structure. The dynamic response of a highway bridge is a complex phenomenon and it is less understood for curved bridges. During the past decades, various studies have attempted to study the dynamic response of curved bridges under moving truck loads. For instance, Billing (1984) presented the outcomes from a series of dynamic tests of 27 bridges in Ontario, Canada.

The datasets were obtained from more than 100 truck crossings for each bridge. It was pointed out bridge frequencies identified under a single truck load are typically larger than design estimations. A similar study was conducted in Switzerland (Cantieni, 1983). Later, Kim et al. (1996) presented the results from truck load tests conducted on seven bridges in the city of Detroit, Michigan. It was concluded truck loads on bridges are strongly

site specific, even within the same geographic area. Senthilvasan et al. (2002) conducted a truck load test on the Turbot Street Bridge, a curved bridge in Australia, using a five-axle truck. It was found the deflections and strains (due to bending moments), are not amplified by the same amount. An important observation they made is the dynamic response not always increases with the speed of the vehicle, but it depends on the ratio of the vibration period to the traverse time. Brady et al. (2006) discussed the results from a truck load test on a simply supported bridge in Slovenia. More recently, Huang (2008) studied the deflection of a curved bridge under moving truck loads.

This paper aims to contribute the body of literature for the study of bridge response under traffic loads. The paper presents the findings of a series of vehicle-crossing tests conducted on the Fairview Road On-Ramp (FRO) bridge, located in Southern California, USA. The effect of truck speed and a sudden stop on the modal identification of the bridge structure is investigated.

* Corresponding author. Tel.: +90-462-3772628 ; Fax: +90-462-3772606 ; E-mail address: akkose@ktu.edu.tr (M. Akköse)

2. Frequency Domain Decomposition (FDD) Technique

The main problem associated with forced vibration tests on bridges, buildings, or dams stems from the difficulty in exciting the most significant modes of vibration in a low range of frequencies with sufficient energy and in a controlled manner. Fortunately, recent technological developments in transducers and analog-to-digital (A/D) converters have made it possible to accurately measure the very low levels of dynamic response induced by ambient excitations like wind or traffic. This has stimulated the development of output-only modal identification methods. Therefore, the performance of output-only modal identification tests became an alternative of great importance in the field of civil engineering. This allows accurate identification of modal properties of large structures at the commissioning stage or during their lifetime without interruption of normal traffic. Ambient excitation usually provides multiple inputs and a wide-band frequency content thus stimulating a significant number of vibration modes. For simplicity, output-only modal identification methods assume that the excitation input is a zero-mean Gaussian white noise. This means that real excitation can be expressed as the output of a suitable filter excited with white noise input. Some additional computational poles without physical meaning appear as a result of the white noise assumption (Cunha and Caetano, 2006).

Output-only modal identification of a civil infrastructure system is associated with the identification of its modal parameters. In the analysis the loads subjected to the system are unknown and the modal identification has to be carried out based on the responses only. Classically, forced vibration is applied to the structures where the applied excitation (input) can be measurable. However, it is often to face the case where the input excitation cannot be measured, i.e. ambient/traffic induced vibration. In such cases it is impractical, if not impossible to measure the excitation forces. Hence, the system identification techniques applied for the identification of modal parameters are separated in two main groups known as output-only and input-output techniques (Brincker et al., 2000).

The Frequency Domain Decomposition (FDD) was first introduced by Brincker et al. (2000). The FDD technique takes the singular value decomposition (SVD) of the spectral matrix which is decomposed into a set of auto spectral density functions, each corresponding to a single degree of freedom (SDOF) system. The results of the FDD are exact when the input excitation is white noise, the structure is lightly damped and when the mode shapes of close modes are geometrically orthogonal. If these assumptions are not satisfied the decomposition into SDOF systems is approximate, but still the results are significantly accurate.

2.1. Theoretical basis of the FDD technique

The relationship between the unknown inputs $x(t)$ and the measured responses $y(t)$ can be expressed as

$$G_{yy}(\omega) = \bar{H}(\omega)G_{xx}H(\omega)^T, \quad (1)$$

where G_{xx} is the (rxr) Power Spectral Density (PSD) matrix of the input, r is the number of inputs, $G_{yy}(\omega)$ is the (mxm) PSD matrix of the responses, m is the number of responses, $H(\omega)$ is the $(m \times r)$ Frequency Response Function (FRF) matrix and “—” and T denote complex conjugate and transpose, respectively. The FRF can be written in partial fraction, i.e. pole/residue form

$$H(\omega) = \sum_{k=1}^n \frac{R_k}{\omega - \lambda_k} + \frac{\bar{R}_k}{\omega - \bar{\lambda}_k}, \quad (2)$$

where n is the number of modes, λ_k is the pole and R_k is the residue given by

$$R_k = \phi_k \gamma_k^T, \quad (3)$$

where ϕ_k and γ_k are the mode shape and the modal participation vectors, respectively. Usually, during experimental modal analysis using ambient/traffic vibration the inputs are unknown. Suppose the input is white noise, i.e. a random signals containing equal power within a fixed bandwidth at any center frequency, its PSD is a constant matrix, i.e. can be written as $G_{xx} = C$, then Eq. (1) becomes

$$G_{yy}(\omega) = \sum_{k=1}^n \sum_{s=1}^n \left[\frac{R_k}{\omega - \lambda_k} + \frac{\bar{R}_k}{\omega - \bar{\lambda}_k} \right] C \left[\frac{R_s}{\omega - \lambda_s} + \frac{\bar{R}_s}{\omega - \bar{\lambda}_s} \right]^H, \quad (4)$$

where superscript H denotes a complex conjugate and transpose. Multiplying the two partial fraction factors and making use of the Heaviside partial fraction theorem, after some mathematical manipulations, the output PSD can be reduced to a pole/residue form as follows

$$G_{yy}(\omega) = \sum_{k=1}^n \frac{A_k}{\omega - \lambda_k} + \frac{\bar{A}_k}{\omega - \bar{\lambda}_k} + \frac{B_k}{-\omega - \lambda_k} + \frac{\bar{B}_k}{-\omega - \bar{\lambda}_k}, \quad (5)$$

where A_k is the k th residue matrix of the output PSD. As for the output PSD itself the residue matrix is an (mxm) hermitian matrix and is given by

$$A_k = R_k C \left(\sum_{s=1}^n \frac{\bar{R}_s^T}{-\lambda_k - \bar{\lambda}_s} + \frac{R_s^T}{-\lambda_k - \lambda_s} \right). \quad (6)$$

The contribution to the residue from the k th mode is given by

$$A_k = \frac{R_k C \bar{R}_k^T}{2\alpha_k}, \quad (7)$$

where α_k is minus the real part of the pole $\lambda_k = -\alpha_k + j\omega_k$. As it appears this term becomes dominating when the damping is light, and, thus, is the case of light damping, the residue becomes proportional to the mode shape vector

$$A_k \propto R_k C \bar{R}_k^T = \phi_k \gamma_k^T C \gamma_k \phi_k^T = d_k \phi_k \phi_k^T, \quad (8)$$

where d_k is a scalar constant. At a certain frequency ω only a limited number of modes will contribute significantly,

typically one or two modes. Let this set of modes be denoted by $Sub(\omega)$. Thus, in the case of a lightly damped structure, the response spectral density can always be written

$$G_{yy}(\omega) = \sum_{k \in Sub(\omega)} \frac{d_k \phi_k \phi_k^T}{\omega - \lambda_k} + \frac{\bar{d}_k \bar{\phi}_k \bar{\phi}_k^T}{\omega - \bar{\lambda}_k}. \quad (9)$$

This is a modal decomposition of the spectral matrix. The expression is similar to the results one would get directly from Eq. (1) under the assumption of independent white noise input, i.e. a diagonal spectral input matrix.

2.2. FDD identification algorithm

In the FDD identification, the first step is to estimate the PSD matrix. The estimate of the output PSD $\hat{G}_{yy}(\omega)$ known at discrete frequencies $\omega = \omega_i$ is then decomposed by taking the Singular Value Decomposition (SVD) of the matrix

$$\hat{G}_{yy}(\omega) = U_i S_i U_i^H, \quad (10)$$

where the matrix $U_i = [u_{i1}, u_{i2}, \dots, u_{im}]$ is a unitary matrix holding the singular vectors u_{ij} , and S_i is a diagonal matrix holding the scalar singular values s_{ij} . Near a peak corresponding to the k th mode in the spectrum this mode, or maybe a possible close mode, will be dominating. If only the k th mode is dominating there will only be one term in Eq. (9). Thus, in this case, the first singular vector u_{i1} is an estimate of the mode shape

$$\hat{\phi} = u_{i1}, \quad (11)$$

and the corresponding singular value is the auto power spectral density function of the corresponding single degree of freedom system, refer to Eq. (9). This PSD function is identified around the peak by comparing the mode shape estimate $\hat{\phi}$ with the singular vectors for the frequency lines around the peak. As long as a singular vector is found that has a high modal assurance criterion (MAC) value with $\hat{\phi}$, the corresponding singular value belongs to the SDOF density function.

From the piece of the single degree of freedom (SDOF) density function obtained around the peak of the PSD, the natural frequency and the damping can be obtained. The piece of the SDOF PSD was taken back to the time domain by an Inverse Fast Fourier transform (IFFT), and the frequency and the damping was simply estimated from the crossing times and the logarithmic

decrement of the corresponding SDOF autocorrelation function.

In the case where two modes are dominating, the first singular vector will always be a good estimate of the mode shape of the strongest mode. However, in the case where the two modes are orthogonal, the first two singular vectors are unbiased estimates of the corresponding mode shape vectors.

In the case where the two modes are not orthogonal, the bias on the mode shape estimate of the dominant mode will typically be small, but the bias on the mode shape estimate of the weak mode will be strong. Thus, one has to estimate the mode shapes for the two close modes at two different frequency lines, one line where the first mode is dominant and another frequency line where the second mode is dominant.

3. Description of Bridge, Monitoring System and Vehicle Crossing Tests

3.1. Description of the Fairview Road On-Ramp (FRO) Bridge

The Fairview Road On-Ramp Overcrossing (FRO) Bridge (Figs. 1, 2) is located in the city of Costa Mesa on the Interstate 405, one of the busiest routes in Southern California. The FRO Bridge is a four-span and one-lane continuous concrete box girder bridge. In plan the bridge is slightly curved with double curvature and radius of curvature of 600m (1,968.5ft). Summary plan and section details are shown in Fig. 3. The length of the bridge is 224m (735ft) along the "F2" line, in which the lengths of spans running from south to north are 52.5, 59.5, 59.5 and 52.5m (172.2, 195.2, 195.2 and 172.2ft), respectively. The super-structure consists of a three-cell cast-in-place pre-stressed and post-tensioned box girder which is aligned 6% to the horizontal. The deck is supported on two monolithic columns and sliding bearings at opposite abutments. Concrete traffic barriers are approximately 0.8m (1.75ft) high, attached to the outer edges of the road.

The sub-structure consists of three single column bents and two tall-seat type abutments. The main bent reinforcement is anchored in solid concrete diaphragms filling the girder void at bent locations, providing continuity between column and box girder. The columns have circular cross-sections with 2.14m (7ft) as the diameter. The bents are founded on square RC pad footings and the abutments are supported on rectangular footings.



Fig. 1. A view of the Fairview Road On-Ramp Overcrossing (FRO) Bridge.



Fig. 2. A close look of the Fairview Road On-Ramp Overcrossing (FRO) Bridge.

3.2. FRO Bridge monitoring system

The FRO Bridge is instrumented with a total of 21 accelerometers (Fig. 4). The accelerometers are either uni-, bi- or tri-axial force-balance servo-type accelerometers. An easy access to the data recorder is possible since it is installed on the ground below the deck at the beginning of the bridge. More details on the instrumentation can be found in Gomez (2011).

3.3. Description of vehicle crossing tests on FRO Bridge

A water truck with capacity of 2,000 gal, was used in the vehicle crossing tests (Fig. 5). At full capacity the truck has a gross vehicle weight of 138 kN. This weight was distributed as 49 kN at the front axle and 89 kN at the rear axle. The distance from the front axle to the rear axle is 3.96m. Although this truck is not one of the heaviest vehicles that could potentially pass on the FRO Bridge, it has a considerable mass to induce an adequate bridge response.

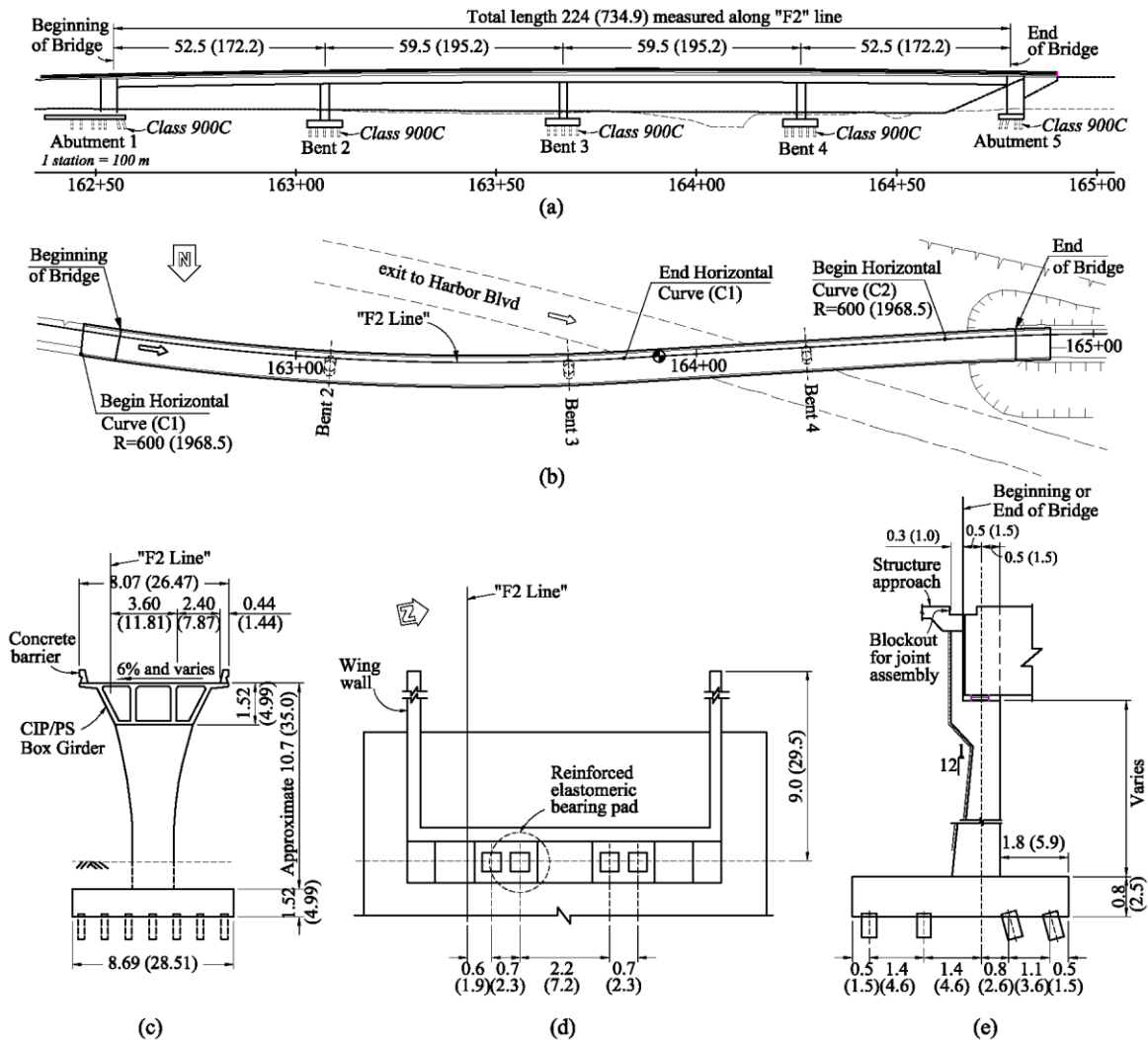


Fig. 3. Structural details of the Fairview Road On-Ramp Overcrossing (FRO) Bridge: (a) elevation; (b) plan view; (c) bent typical section; (d) abutment layout plan view; (e) typical abutment section (dimensions in m (ft)).

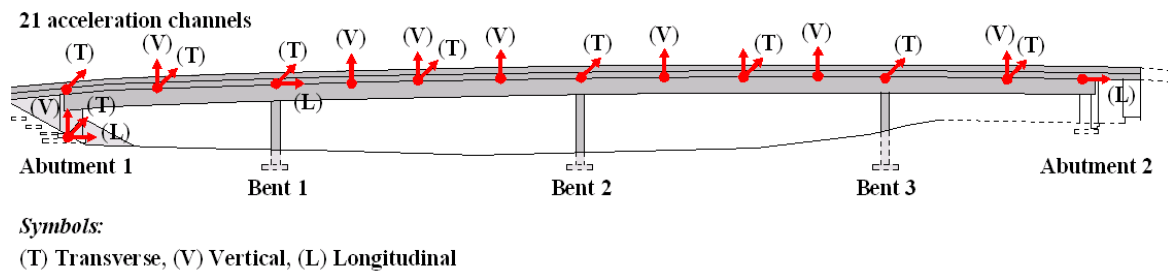


Fig. 4. Sensor layout at FRO Bridge.

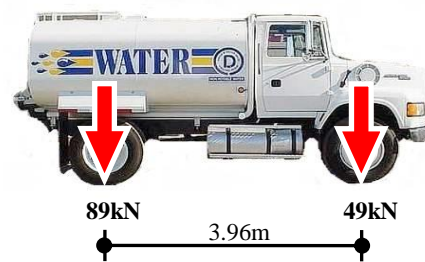


Fig. 5. Truck weight and dimensions.

During the vehicle-crossing tests (Fig. 6), after the bridge is closed to public traffic, the truck entered the beginning of the bridge (Abutment 1) with a constant speed of 8 km/h (5 mph) and made a complete stop at the middle of the second span. After one minute, the truck started moving again at a speed of approximately 8 km/h until it arrived at the middle of the third span where it made a second complete stop. After one minute, the truck resumed the trip and left the bridge at a speed of approximately 8 km/h. Afterwards, the truck made a U-turn and entered from the end of the bridge (Abutment 5) and made two stops, one minute each, at the same locations as going forward (see Fig. 6). Then, the test vehicle exits the bridge at speed of 8 km/h and completes its first round trip.

Another test consisted in driving the test vehicle at a speed of approximately 72-81 km/h (45-50 mph). When the vehicle arrived at the middle of the second span, the breaks were suddenly applied to generate an impact load on the bridge. Then, the truck proceeded at 8 km/h and left the bridge. Next, the truck made a U-turn for the final trip. In the last trip, the truck entered at the end of bridge and accelerated to reach a speed of approximately 48-56 km/h (30-35 mph). Another sudden break was applied at the middle of the third span. The test vehicle resumed the trip at 8 km/h and left the bridge.

4. Results and Discussion

Fig. 7 shows the acceleration time-history response at sensor locations during the vehicle-crossing tests. It was found 7 accelerometers (#'s 9, 14, 17-21) were malfunctioning at the time of the tests. Since the accelerometers

were installed inside the box girder, it was not possible to access for a detailed inspection of the sensors and the reasons for the malfunctioning were unknown. Therefore, the remaining 14 accelerometers were used to study the bridge response. Despite the malfunctioning sensors, it was still possible to attain an accurate identification of the modal parameters of the bridge. The remaining sensors provided the adequate information in order to identify the modes of vibration with high confidence.

In Fig. 7, the bridge response acceleration time-histories were subdivided into nine groups, identified by colors, according to the level of acceleration. It can be observed the magnitude of the vertical response of the bridge was drastically increased (about 200%) for the tests where a sudden stop of the test vehicle was applied. Afterwards, each group of accelerations was analyzed to identify the bridge modal parameters.

4.1. Bridge modal identification

The frequency domain decomposition (FDD) was applied to the acceleration datasets to identify bridge modal parameters. The FDD technique was introduced by Brincker et al. (2000) as an alternative to other frequency domain system identification techniques. The FDD technique has been widely used for system identification of bridges in recent years (Kim et al., 2003; Feng et al., 2004; Chen et al., 2006; Gomez et al., 2011; Gomez, 2011).

The power spectral density functions used by the FDD were estimated using Hanning windows with 60% overlap. In order to reduce background noise, a butter-worth infinite impulse response filter of order 8 was applied to

the data with a pass-band defined by a lower frequency of 1 Hz and a higher frequency of 10 Hz. The FDD results are shown in Fig. 8. The identification of the natural frequencies is presented for the nine groups of bridge re-

sponses separately. The natural frequencies are identified at approximately 1.465, 2.002, 2.295, 2.881, and 3.076 Hz. It can be seen that natural frequencies are consistent for each set of data.

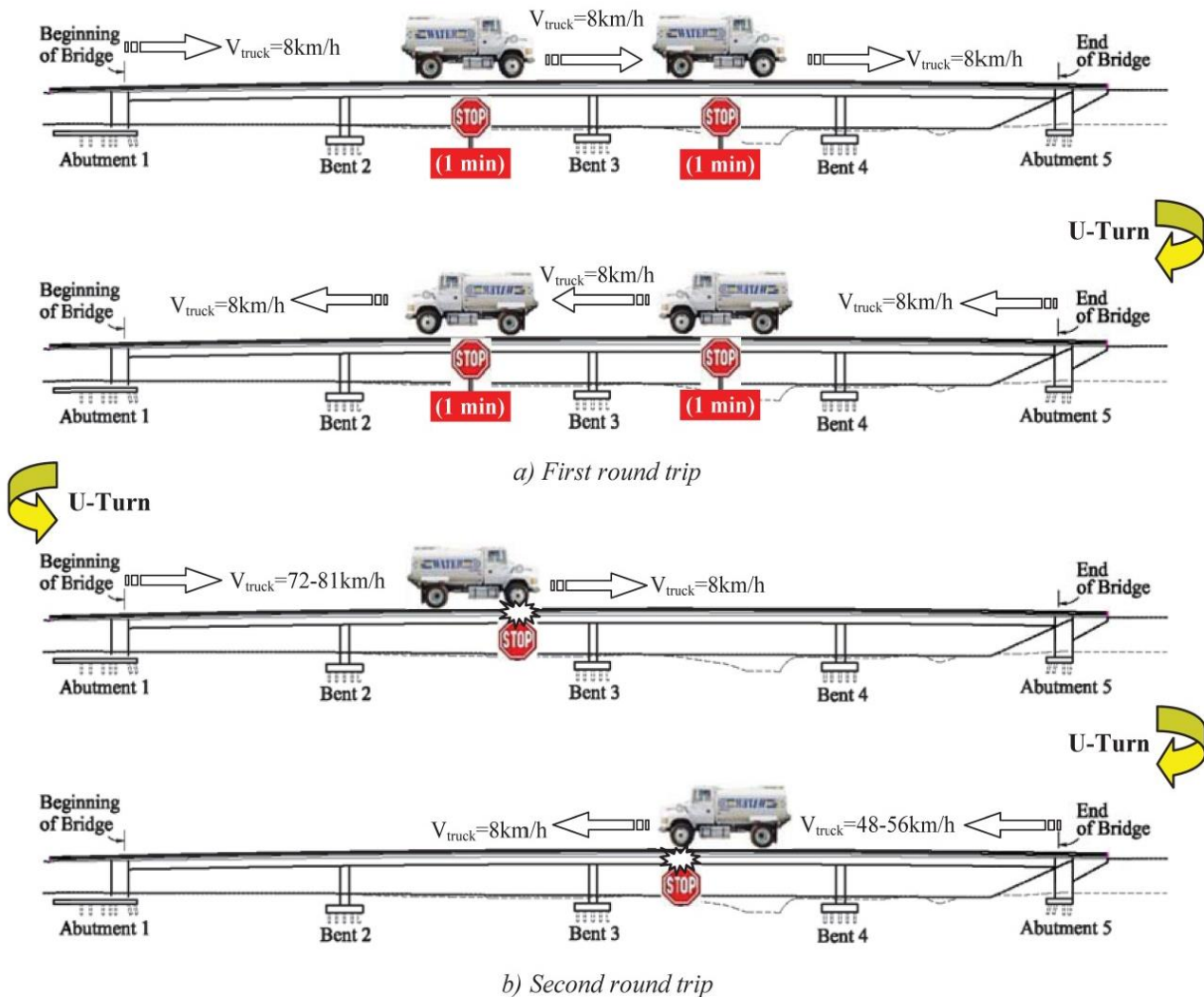


Fig. 6. Description of vehicle crossing tests (total test duration was approximately 18 minutes).

In addition to bridge natural frequencies, partial mode shapes (as the bridge is instrumented at discrete locations only) are plotted for the first three modes (see Fig. 9). Although the first three modes exhibit some combination of vertical and horizontal motions, it is clear that the first mode ($f_1 = 1.465$ Hz) is a lateral rocking mode about the longitudinal axis of the bridge with the three bents in phase. This mode is clearly identified from the time history segment from 610 s to 800 s (cyan color in Fig. 7). During this time segment no vehicle was on the bridge. It is noted this mode is not always identified (or it has a low peak amplitude in the frequency plots) because in most of the data sets the data contain the response of the bridge due to the truck load, which predominantly excites the vertical modes. This is clearly observed in the next two modes of vibration ($f_2 = 2.002$ Hz and $f_3 = 2.295$ Hz), which are a combination of vertical bending and torsion of the bridge deck.

From the results presented above, it can be sensibly argued the passing of the truck rendered difficult to identify the first bridge frequency. Conversely, the vehicle tests improved the identification of higher vibration modes. This is because the truck tends to excite the bridge vertical response, which is associated with higher modes of vibration, especially when a sudden stop of the vehicle occurs (magenta and blue last two segments, from 800 s to 1098 s in Fig. 7).

Another observation from the identification results is the natural frequencies are practically the same for different speeds of the truck as different segments in the time histories were recorded for different speeds as described earlier. Therefore, the modes of vibration were not influenced by truck speeds, which ranged from 8 to 80 km/h. Further studies are recommended to study the effect of truck speed on the modal identification by using higher vehicle velocities.

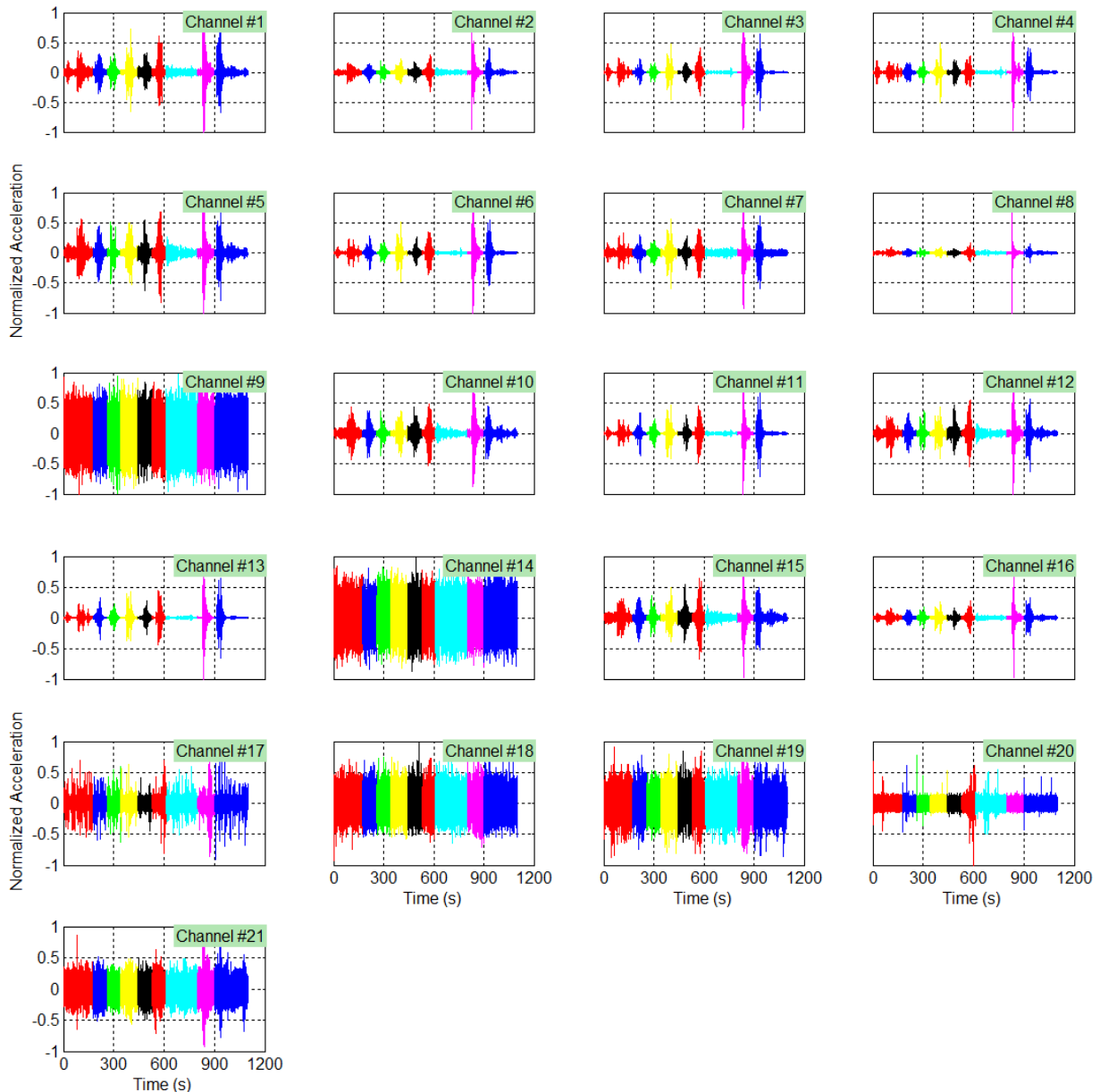


Fig. 7. Normalized acceleration time-history response at sensors during the vehicle tests.

5. Conclusions

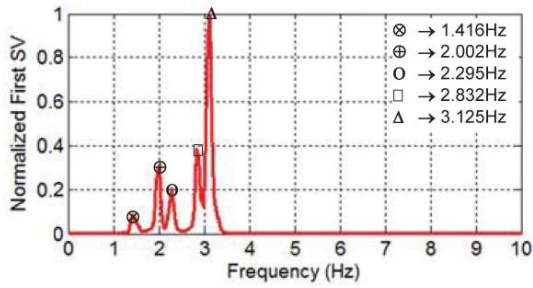
In this study, the findings of a series of vehicle crossing test on a concrete bridge are presented. Acceleration response datasets were recorded during the tests. The natural frequencies of the bridge were determined using the frequency domain decomposition (FDD) technique for all datasets. The identification results show that the first frequency is associated with lateral mobilization of the deck and bending of the columns whereas higher modes are associated with the vertical and torsional mobilization of the deck.

It was observed that the passing of the truck renders difficult to identify the first bridge frequency. This is because the first bridge frequency is associated with bending of the columns and lateral mobilization of the deck. Conversely, the vehicle tests improved the identification of higher vibration modes because these are associated

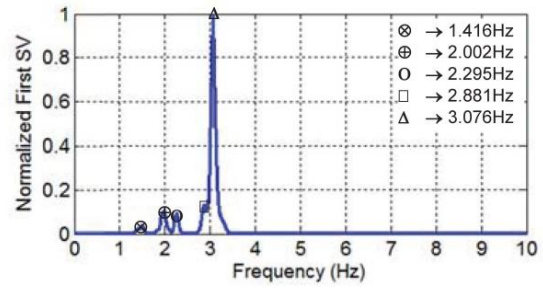
with vertical bridge response. This is more apparent for the crossing vehicle tests where a sudden stop was applied inducing a bigger vertical force on the bridge. In this case, the magnitude of the vertical response of the bridge is drastically increased (about 200%).

Since no change in the identification results was observed due to an increase in truck speed, it is concluded the amplification of the magnitude of the bridge response due to an increased vertical load (heavier vehicles or a sudden stop), exceeds any velocity effect.

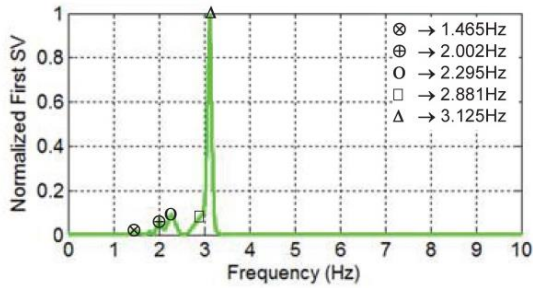
It is the authors' opinion that carefully conducted vehicle-crossing tests provide detailed information about the bridge structure dynamics in the vertical direction. However, to identify lower modes, no vehicle on the bridge is preferred. Moreover, much higher truck velocities than those attained in this study (a maximum of approximately 80 km/h) are recommended in order to study any effects on bridge response.



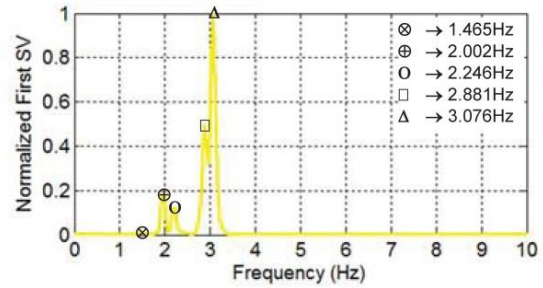
For 1st group data (first red color section in Fig. 6)



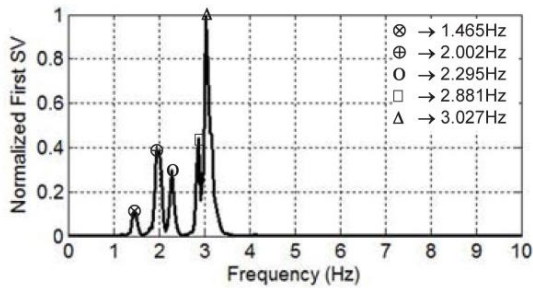
For 2nd group data (first blue color section in Fig. 6)



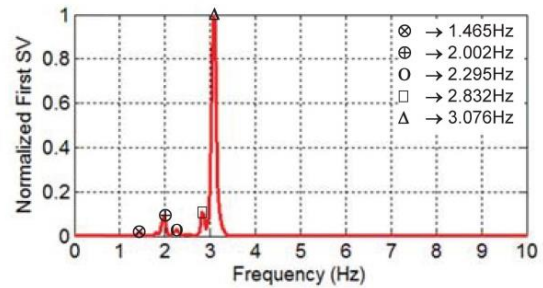
For 3rd group data (green color section in Fig. 6)



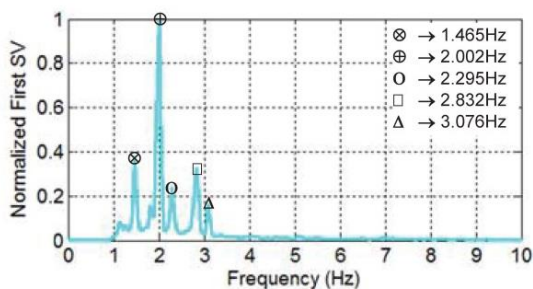
For 4th group data (yellow color section in Fig. 6)



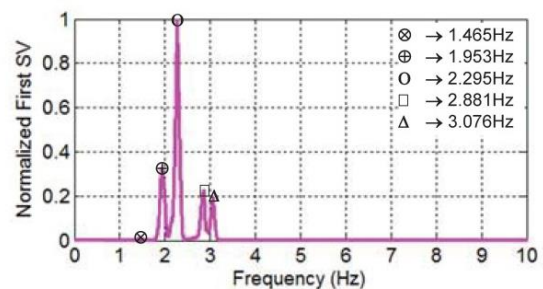
For 5th group data (black color section in Fig. 6)



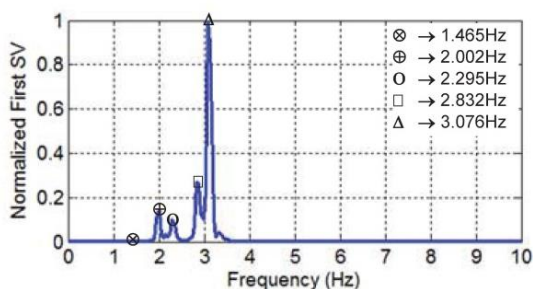
For 6th group data (second red color section in Fig. 6)



For 7th group data (cyan color section in Fig. 6)



For 8th group data (magenta color section in Fig. 6)



For 9th group data (second blue color section in Fig. 6)

Fig. 8. Normalized first SV obtained from FDD applied to data recorded during vehicle crossing tests.

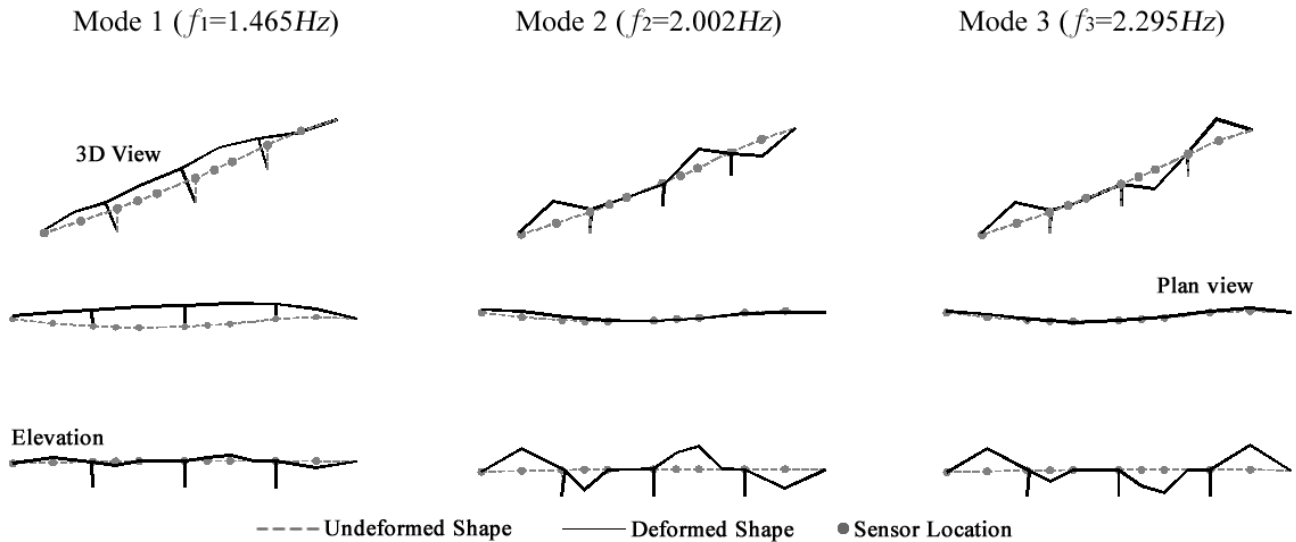


Fig. 9. Identified partial mode shapes of the FRO Bridge.

Acknowledgements

This research was supported by the Scientific and Technical Research Council of Turkey (TUBITAK) under the 2219-Foreign Postdoctoral Research Scholarship Program. The authors also wish to thank the support of the California Department of Transportation.

REFERENCES

- Billing JR (1984). Dynamic loading and testing of bridges in Ontario. *Canadian Journal of Civil Engineering*, 11(4), 833-843.
- Brady SP, O'Brien EJ, Žnidarič A (2006). Effect of vehicle velocity on the dynamic amplification of a vehicle crossing a simply supported bridge. *Journal of Bridge Engineering*, 11(2), 241-249.
- Brincker R, Zhang L, Andersen P (2000). Modal identification from ambient response using frequency domain decomposition. *Proceedings of the 18th International Modal Analysis Conference (IMAC18)*, Society for Experimental Mechanics, San Antonio, TX, USA, 625-630.
- Cantieni R (1983). Dynamic load tests on highway bridges in Switzerland. Rep. No. 211, *Eidgenössische Material-prüfungs-und Versuchsanstalt (EMPA)*, Dübendorf, Switzerland.
- Chen Y, Feng MQ, Tan CA (2006). Modeling of traffic excitation for system identification of bridge structures, *Computer-Aided Civil and Infrastructure Engineering*, 21(1), 57-66.
- Feng MQ, Kim DK, Yi J-H, Chen Y (2004). Baseline models for bridge performance monitoring, *Journal of Engineering Mechanics*, 130(5), 562-569.
- Gomez HC (2011). System identification of highway bridges using long-term vibration monitoring data, *Ph.D. thesis*, University of California, Irvine, USA.
- Gomez HC, Fanning PJ, Feng MQ, Lee S (2011). Testing and long-term monitoring of a curved concrete box girder bridge, *Engineering Structures*, 33(10), 2861-2869.
- Huang D (2008). Dynamic loading of curved steel box girder bridges due to moving vehicles. *Structural Engineering International*, 18(4), 365-372.
- Kim CY, Jung DS, Kim NS, Kwon DS, Feng MQ (2003). Effect of vehicle weight on natural frequencies of bridges measured from traffic-induced vibration. *Earthquake Engineering and Engineering Vibration*, 2(1), 109-115.
- Kim S, Sokolik A, Nowak A (1996). Measurement of truck load on bridges in Detroit, Michigan, area. Transportation Research Record: *Journal of the Transportation Research Board*, 1541(1), 58-63.
- Senthilvasan J, Thambiratnam DP, Brameld GH (2002). Dynamic response of a curved bridge under moving truck load. *Engineering Structures*, 24(10), 1283-1293.